Conversion Loss in GaAs Schottky-Barrier Mixer Diodes

THOMAS W. CROWE, STUDENT MEMBER, IEEE, AND ROBERT J. MATTAUCH, FELLOW, IEEE

***Abstract*—In this paper, the intrinsic conversion loss of GaAs Schottky-barrier mixer diodes is analyzed in light of a more accurate diode model. This analysis resolves the discrepancy between the predictions of an earlier intrinsic conversion loss model and experimental results. In particular, it is shown that a) cryogenic cooling should not degrade the conversion loss, and b) the diode diameter can be smaller than previously predicted before conversion-loss degradation begins to occur. Evidence is also presented which indicates that mixer diodes must be pumped beyond flat-band if the minimum possible conversion loss is to be obtained. A more complete model of the conversion loss, which includes the parasitic circuit elements, is discussed and found to be in agreement with the qualitative results of the intrinsic conversion-loss model.**

I. Introduction

As THE NEED FOR millimeter and submillimeter wavelength receivers continues to grow, the optimization of Schottky-barrier mixer diodes for these higher frequencies becomes more important. Diode optimization requires the minimization of both noise and conversion loss. Noise reduction is often achieved by cooling the mixer to cryogenic temperatures [1]. In well-designed mixers, this leads to as much as a factor of four decrease in shot noise. For modeling purposes, conversion loss may be divided into intrinsic loss L_0 and parasitic loss L_p. Intrinsic loss is the amount of loss that would occur if there were no parasitic elements, i.e., series resistance and junction capacitance, in the diode. Thus, the intrinsic loss is caused by the finite junction conductance (it is not an ideal switch) and by nonoptimum impedance matching. Parasitic loss is defined as the increase in conversion loss due to the presence of nonzero parasitic elements, and is generally approximated by [2], [3]

$$L_p = (1 + R_s/R_{IF})(1 + R_s/R_{RF} + \omega^2 C_j^2 R_{RF} R_s). \quad (1)$$

This equation assumes that the diode, when pumped by the local oscillator, can be modeled as a small-signal linear circuit element with constant junction capacitance C_j, constant series resistance R_s, and equivalent impedances R_{RF} and R_{IF} at the signal and image frequencies, respectively. The intrinsic conversion loss has previously been examined in an important paper by McColl [4]. In that work, the intrinsic diode (without parasitic elements) was placed in a Y-type mixer circuit,[1] and expressions for the conversion loss were derived using classical mixer theory of Torrey and Whitmer [5]. This model has predicted that the intrinsic conversion loss will become prohibitively large if the diode is cryogenically cooled to reduce noise, or if the diode diameter is decreased to minimize parasitic capacitance. Although these conclusions have not been verified experimentally (see for example [6]–[8]), this theoretical model has often been cited in the literature [9]–[11]. The study reported on here has resolved this discrepancy through the use of a more accurate model of the Schottky diode.

In Section II, the model of the Schottky diode is evaluated, with special attention devoted to its behavior at high biases. The intrinsic conversion loss model is then reevaluated in Section III. It is shown that intrinsic conversion-loss degradation due to cryogenic cooling should not occur, and it is predicted that the device diameter can be significantly smaller than previously predicted without conversion-loss degradation. Furthermore, it is shown that the intrinsic conversion loss is minimized only when the instantaneous diode current is allowed to exceed that occurring for the flat-band condition for part of the LO cycle. Throughout this paper, the flat-band condition is defined as the case where the forward voltage applied to the junction is large enough to shrink the depletion region length to zero. At this point the potential barrier from the semiconductor to the metal is reduced to zero and the conduction band is gradient free (or flat) provided that the electric field in the undepleted epitaxial layer is neglected.

The intrinsic conversion loss sets a lower limit on the total conversion loss since it neglects losses due to the parasitic circuit elements. Recently, a more accurate technique has been developed to investigate the conversion loss with the parasitic elements included [12], [13]. In general, this technique requires three major steps:

1) complete characterization of the diode mount so that the impedances seen by the diode at all relevant frequencies are known;
2) solution of the nonlinear circuit problem to find the junction voltage and current produced by the local oscillator (LO) as functions of time. This yields the conductance and capacitance of the diode as functions of time $G(t)$ and $C(t)$;
3) Fourier analysis of $G(t)$ and $C(t)$, so that the coefficients of the small-signal conversion matrix, and, hence, the conversion loss, can be determined.

In Section IV, this analysis is used with two simplifying

Manuscript received October 25, 1985; revised February 24, 1986. This work was sponsored in part by the National Science Foundation under Contract ECS-8022937-02.
The authors are with the Department of Electrical Engineering, University of Virginia, Thornton Hall, Charlottesville, VA 22901.
IEEE Log Number 8608676.

[1]All frequencies above the upper sideband ($\omega_{LO} + \omega_{IF}$) are short circuited at the diode terminals (see [17]).

0018-9480/86/0700-0753$01.00

assumptions. In particular, an idealized diode mount, which short circuits the diode terminals at all frequencies above the upper sideband, and a sinusoidal local oscillator voltage across the diode are assumed. This model allows consideration of the effect of the diode parasitic elements (R_s and C_j), and, therefore, should give a meaningful indication of the performance of real mixer diodes.

A set of diode parameters from a typical diode designed for cryogenic operation and produced in our lab was analyzed by this numerical technique. The results indicated that cryogenic cooling will not significantly increase the expected total conversion loss, and the minimum loss will be obtained only if the LO power is large enough so that the flat-band condition is exceeded. These conclusions are in agreement with those of our new intrinsic conversion loss model and also agree with common experimental results [6]–[8].

II. The Schottky Diode

A. Room Temperature

At room temperature, a Schottky diode formed on material of typical doping density (between 2×10^{16} and 3×10^{17}cm^{-3}) is best modeled as a thermionic emitter. Analysis of this case leads to the Richardson equation [14]

$$I = A^*ST^2\exp\left(\frac{V_a-\psi-IR_s}{V_0}\right) \tag{2}$$

where

- S diode area, cm^2,
- A^* the modified Richardson constant, A/cm^2/K^2,
- T diode temperature, K,
- V_a the total applied bias, V,
- ψ the barrier height, V,
- R_s the diode series resistance,
- V_0 ηkT/q
- k the Boltzmann const., J/K,
- q electronic charge, C,
- η the diode ideality factor.

The flat-band current I_{FB} is the forward current at the bias point where the depletion region width becomes zero. The barrier height ψ and the flat-band potential V_{FB} are defined in Fig. 1. When the voltage applied to the junction is equal to V_{FB}, the flat-band condition is obtained.

This model assumes a Maxwell-Boltzmann electron distribution and considers only the emission of electrons over the barrier. Thus, both electron tunneling and hot electron effects (caused by the nonzero electric field in the series resistance) are ignored. At room temperature, these effects play only a minor role and this model is quite appropriate.

The diode junction capacitance is approximated as

$$C_j = S\left(\frac{q\epsilon N}{2(V_{FB}-V_a)}\right)^{1/2}(1+3x/d), \qquad I < I_{FB} \tag{3}$$

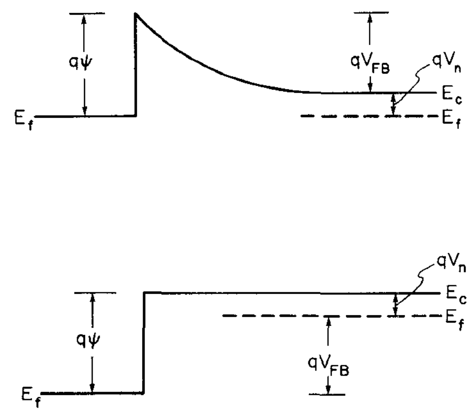

(b)

Fig. 1. Band diagram of a Schottky-barrier diode showing the barrier height ψ, the flat-band potential V_{FB}, and the potential difference between the Fermi level and the conduction band in the undepleted semiconductor V_n. (a) Zero bias and (b) $V_j = V_{FB}$, the flat-band condition.

where

- ϵ the permittivity of the semiconductor, F/cm,
- N the doping density in the depletion region, cm^{-3},
- x the depletion region width, cm,
- d the diode diameter, cm,

and all other terms are as previously defined. The rightmost term accounts for fringing effects [15]. The exact capacitance law is difficult to derive due to the fringing effects, and the invalidity of the depletion approximation near flat-band. However, the type of capacitance law given by (3) is verified by experimental evidence [16], and is believed to be a valid approximation when $V_j < V_{FB}$.

At this point it is convenient to note that the diode $I-V$ characteristic depends on the value of the barrier height ψ, while the $C-V$ characteristic depends on the flat-band potential, V_{FB}. As was shown in Fig. 1, these values differ by an amount defined as V_n, and cannot, in general, be assumed equal.

The behavior of the diode for voltages near and beyond flat-band is often misunderstood. Although the small-signal junction capacitance theoretically approaches infinity as V_j approaches V_{FB}, it must be realized that the junction capacitance occurs solely due to the storage of charge in the depletion region. Thus, since the total amount of charge stored is always finite, the junction capacitance, $C_j = dQ/dV$, is large for only a very small range of voltage. If the total voltage applied to the diode is allowed to exceed the flat-band condition, the depletion region will become neutralized and the junction capacitance and resistance will no longer exist. At this point, the current is limited solely by the diode series resistance. Thus, biasing beyond flat-band will yield the minimum possible total diode impedance (namely R_s). Previous investigations of resistive mixers have shown that the minimum conversion loss is obtained only when the mixer diode resistance is allowed to swing between the maximum and the minimum possible values [17]. We would expect, therefore, that to minimize the conversion loss the diode current should be allowed to exceed the flat-band condition for part of the LO cycle. This conclusion, which is supported in the following sections, indicates that limiting the diode current below flat-band is overly restrictive and leads to pessimistic approximations of the conversion loss.

The diode characteristics for cases where $I > I_{FB}$ are assumed here to be those of a linear differential resistance given by

$$I = (V_a - V_{FB})/R_s, \qquad I >= I_{FB} \tag{4}$$

$$C_j = 0, \qquad I >= I_{FB}. \tag{5}$$

B. Cooled Diodes

GaAs Schottky diodes are often cooled to cryogenic temperatures to reduce their noise temperature. Extension of the conversion loss analysis to cryogenic temperatures requires that the diode characteristics at these temperatures be evaluated. Previous research has shown that tunneling [18] and hot electron effects [19] become important in cooled diodes. However, the dc current–voltage characteristics can still be modeled in the form

$$I = I_{sat}\exp\left(\frac{V_a - IR_s}{V_0}\right), \qquad I < I_{FB} \tag{6}$$

$$I = (V_a - V_{FB})/R_s, \qquad I >= I_{FB}. \tag{7}$$

At cryogenic temperatures, the values of I_{sat} and V_0 are functions of the diode doping, temperature, and the current density (due to electron heating effects), and must be determined empirically. The junction capacitance in cooled devices behaves in the same way as at room temperature. In the present work, we shall neglect electron heating effects, which tend to alter the $I-V$ and $C-V$ characteristics of cooled devices as flat-band is approached. In the worst case, this approximation will slightly alter the shape of the conductance and capacitance waveforms of the diode without affecting their peak and minimum values. With this approximation, measured values of I_{sat}, V_0, and R_s can be used to approximate the barrier height. The flat-band potential can then be found provided the parameter V_n, defined in Fig. 1, is known. Using Fermi-Dirac statistics, V_n is expressed as [14, p. 17]

$$V_n = \frac{kT}{q} F_{1/2}^{-1}\left(\frac{n\sqrt{\pi}}{2N_c}\right) \tag{8}$$

where $F_{1/2}^{-1}$ is the inverse Fermi function of order $1/2$, n is the free-carrier concentration, and N_c is the effective density-of-states in the conduction band. The variation of the free-electron concentration with temperature must be considered. Although first-order theory predicts carrier freeze-out at cryogenic temperatures, the small ionization energy of donors in moderate to heavily doped GaAs and the small electronic mass prevent this from occurring [20]. Experimental evidence shows that freeze-out is unimportant in GaAs samples doped above $10^{17}\ \text{cm}^{-3}$, and has only a small effect on samples doped in the mid $10^{16}\ \text{cm}^{-3}$ range [21]. If freeze-out is neglected, the value of V_n can be found from (8), and V_{FB} can be found since $V_{FB} = \psi - V_n$.

III. Intrinsic Conversion Loss

The limitations of mixer analysis in terms of the intrinsic and parasitic conversion loss have been discussed in the introduction. However, this approach can give physical insight into the behavior and limitations of mixers, and has been used by McColl [4] to study the behavior of mixers in which the instantaneous applied voltage was constrained so that the flat-band condition was not exceeded. In this section, the intrinsic conversion loss model is reevaluated. However, our model of the Schottky diode (Section II) differs from McColls's model in two important ways. First, the diode barrier height ψ and the flat-band potential V_{FB} are not assumed equal. This has a significant effect on the temperature variation of the intrinsic loss. Second, the forward current is allowed to exceed the flat-band current. This improves substantially the conversion loss of small diameter diodes.

If the mixer element is modeled as an ideal exponential diode, i.e.,

$$I = I_{sat}\exp(V/V_0) \tag{9}$$

where

$$I_{sat} = A^*ST^2\exp(-\psi/V_0) \tag{10}$$

$$V_0 = kT/q \tag{11}$$

the conductance versus time of the sinusoidally pumped diode can be expressed in a Fourier series

$$G(t) = G_0/2 + G_1\cos(\omega_{LO}t) + G_2\cos(2\omega_{LO}t) + \cdots \tag{12}$$

where

$$G_n = 2I_{sat}I_n(V_{LO}/V_0)\exp(V_{dc}/V_0)/V_0. \tag{13}$$

V_{dc} and V_{LO} are the dc bias voltage and the peak amplitude of the sinusoidal local oscillator voltage, respectively, ω_{LO} is the local oscillator frequency, and $I_n(x)$ represents the modified Bessel function of the first kind of order n. Following McColl, the conversion loss, assuming matched source and load, can be expressed as

$$L_{00} = 2\left(1 + \sqrt{1-\zeta}\right)^2/\zeta \tag{14}$$

where

$$\zeta = 2G_1^2/(G_0(G_0 + G_2)). \tag{15}$$

Since G_n depends on V_{LO} and V_{dc}, the matched intrinsic loss, L_{00}, is also a function of the bias condition.

For the sake of analysis we will temporarily maintain the assumption that the maximum diode voltage ($V_{dc} + V_{LO}$) must remain below the point where the depletion region length reaches zero. The maximum diode current I_{max} is then given by the flat-band current I_{FB}. With (2), the maximum current can be expressed as

$$I_{max} = I_{FB} = A^*ST^2\exp\left(\frac{V_{FB} - \psi}{V_0}\right) = A^*ST^2\exp(-V_n/V_0). \tag{16}$$

This equation is in direct conflict with the similar equation

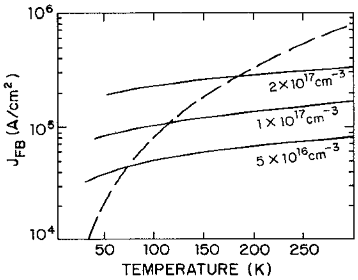

Fig. 2. The forward current density through the junction when $V_j = V_{FB}$ versus diode temperature. Solid lines represent three different free-carrier concentrations, and the dashed line represents the approximation $V_n = 0$.

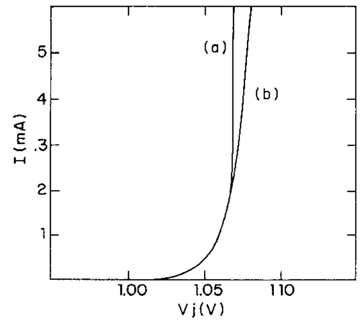

Fig. 4. DC current–voltage characteristics of the diode junction assuming (a) $R_j = 0$ when $I > I_{FB}$ and (b) the junction remains exponential when $I > I_{FB}$. Case (b) overestimates the diode resistance when $I > I_{FB}$.

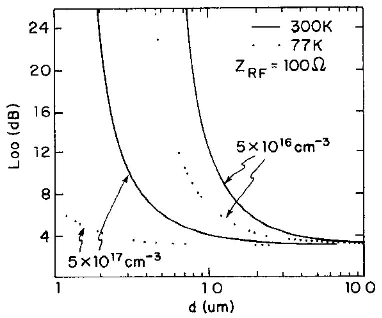

Fig. 3. Matched intrinsic conversion loss L_{00} versus diode diameter assuming $V_{dc} + V_{LO} = V_{FB}$. Results for two different doping densities and temperatures are shown. Decreases in the temperature and increases in the doping density both greatly reduce the intrinsic loss of small diodes. The value of V_{dc} has been chosen so that the RF source (100 Ω) is matched to the intrinsic diode.

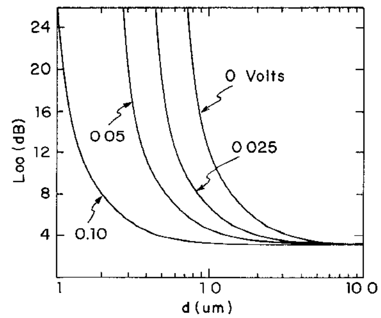

Fig. 5. Matched intrinsic conversion loss versus diode diameter when $V_{dc} + V_{LO}$ is allowed to exceed V_{FB}. The junction is assumed to behave exponentially when $I > I_{FB}$. Values shown are the amounts of excess instantaneous voltage allowed in each case. A small increase in bias greatly reduces the intrinsic loss of small diodes. $T = 300$ K and $N_d = 5 \times 10^{16}$ cm^{-3} are assumed.

in [4] which expressed the maximum current density as $J_{max} = A^*T^2$. This discrepancy occurs because in the previous work the junction voltage which shrinks the depletion region length to zero (V_{FB}) and the barrier height (ψ) were assumed equal. (This is evident when the equations for the $I-V$ and $C-V$ characteristics of that work ([4, eqs. 3 and 19] are considered.) In reality, that work has implicity assumed that the parameter V_n is equal to zero, allowing the omission of the exponential term from (16). However, (8) shows that V_n is actually a function of diode temperature. Thus, it is not accurate to neglect this term when considering the operation of a Schottky diode as a function of temperature. Shown in Fig. 2 is a graph of the flat-band current density J_{FB} versus temperature for three different free-carrier concentrations (solid lines) and for the simplified case where $V_n = 0$ (dashed line). Note that the assumption $V_n = 0$ is valid at only one temperature for each doping density. Also, the variation in J_{FB} with temperature is significantly less than is predicted if $V_n = 0$ is assumed.

Again following McColl, we can plot the intrinsic, matched conversion loss L_{00} versus the diode diameter. However, since V_n is no longer assumed equal to zero, the free-carrier concentration, as well as the temperature, must be considered as a variable parameter. This is shown in Fig. 3. Note that for either of the doping densities shown, the intrinsic loss is decreased when the diode temperature is reduced. This is due to the increased nonlinearity of the cooled device.

As was mentioned previously, the limitation that the forward current must remain below I_{FB} is overly restrictive. Thus, the results shown in Fig. 3 are somewhat pessimistic. A more realistic method of evaluating intrinsic loss is to allow the forward current to exceed the flat-band condition. Ideally, a junction resistance of zero ohms would be used when flat-band is exceeded. However, (12)–(15) are valid only if an exponential $I-V$ characteristic is used. For simplicity, the assumption that the $I-V$ characteristic remains exponential beyond flat-band is used in this analysis. The result of this approximation is shown in Fig. 4 and is slightly pessimistic since it over estimates the junction resistance in the region where $I > I_{FB}$. Results from this calculation for the case that gave the highest loss in Fig. 3 are shown in Fig. 5. The intrinsic loss decreases significantly as the total voltage is allowed to exceed the flat-band voltage value. For all cases investigated, regardless of the doping density and temperature, similar drastic improvements in L_{00} occur when the bias is allowed to exceed the flat-band condition.

IV. Total Conversion Loss

The intrinsic conversion-loss model, presented in the previous section, sets a lower limit on the expected conversion loss of the mixer. However, parasitic elements can add

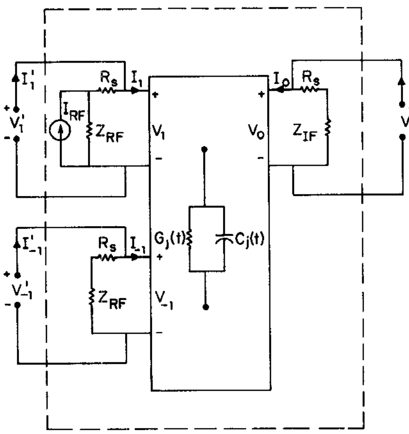

Fig. 6. The small-signal representation of the pumped mixer diode as a linear three-port network with terminations at the RF, IF, and image frequencies. The series resistance is treated as part of the embedding network. The dashed line represents the boundary of the augmented Y-matrix (21).

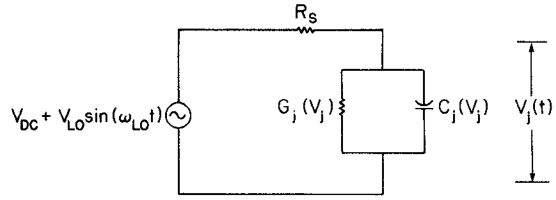

Fig. 7. The large-signal circuit used to evaluate the junction voltage $V_j(t)$ and the junction conductance and capacitance $G_j(t)$ and $C_j(t)$, respectively.

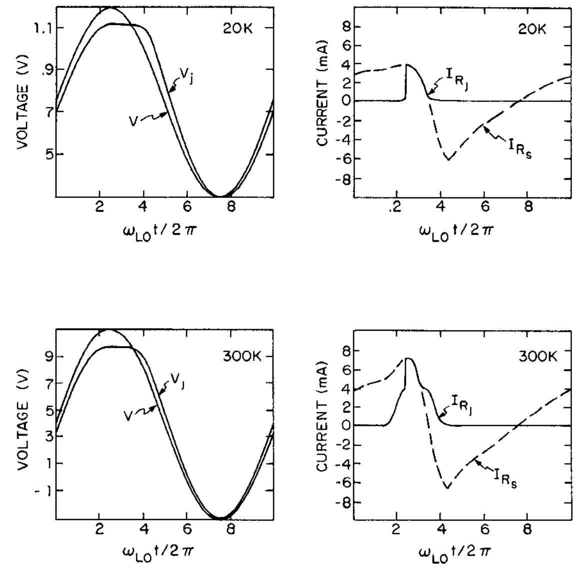

Fig. 8. Typical results from the large-signal analysis of a 1H1 diode showing the diode currents and voltages at 300 K and 20 K for one complete LO cycle. The diode parameters are shown in Table I, and an LO frequency of 300 GHz has been assumed.

greatly to the conversion loss; thus, it is important to consider the effects of cryogenic cooling and diode diameter on the total conversion loss. A more accurate method of evaluating the conversion loss has recently been developed [12], [13]. In these analyses, the diode parasitics are considered, the local oscillator voltage across the junction is evaluated exactly, and the complex embedding impedances at the higher sideband frequencies are considered. Unfortunately, this type of analysis is necessarily complex and requires detailed characterization of the diode mount. For the purposes of this study, an idealized diode mount has been assumed. In particular, the higher order sidebands and LO harmonics are assumed to be short circuited, and a sinusoidal local oscillator voltage across the diode terminals is assumed. This model of the diode mount is the same as that used in the intrinsic conversion-loss analysis. This simplification finds greatest use in the prediction of trends in diode performance as diode parameters are varied. Experimental results will, of course, depend on the diode mount used.

The small-signal circuit diagram for our analysis is shown in Fig. 6. A broad-band case with a matched IF load is assumed and the diode series resistance is considered as a part of the embedding circuit. This greatly simplifies the analysis and does not affect any of the currents and voltages appearing in the series resistance provided that R_s is linear. This approximation is valid provided that the series resistance is linear as compared to the junction resistance, and has been generally accepted in the literature [12], [13]. The admittance of the junction can be expressed by a complex matrix equation of the form

$$\begin{bmatrix} I_1 \\ I_0 \\ I_{-1} \end{bmatrix} = \begin{bmatrix} Y_{11} & Y_{10} & Y_{1-1} \\ Y_{01} & Y_{00} & Y_{0-1} \\ Y_{-11} & Y_{-10} & Y_{-1-1} \end{bmatrix} \cdot \begin{bmatrix} V_1 \\ V_0 \\ V_{-1} \end{bmatrix} \tag{18}$$

where

$$Y_{mn} = G_{m-n} + j\omega_m C_{m-n}$$

and G_p and C_p are the Fourier coefficients of the periodic junction conductance and capacitance given by

$$G_p = \frac{\omega_{LO}}{2\pi}\int_{-\pi/\omega_{LO}}^{\pi/\omega_{LO}} G(t)\exp(-jp\omega_{LO}t)\,dt \tag{19}$$

$$C_p = \frac{\omega_{LO}}{2\pi}\int_{-\pi/\omega_{LO}}^{\pi/\omega_{LO}} C(t)\exp(-jp\omega_{LO}t)\,dt. \tag{20}$$

The subscripts 0, 1, and -1 represent the IF, RF, and image frequencies, respectively. This notation is consistent with that of Saleh, which has been commonly accepted in the literature.

The first step in the analysis is to solve numerically for the diode capacitance and conductance waveforms $C(t)$ and $G(t)$, using the circuit shown in Fig. 7. This is achieved by dividing the local oscillator cycle into n equal intervals of time Δt. Within each interval, the applied voltage $V_{dc} + V_{LO}\sin(\omega_{LO}t)$, is assumed to vary linearly, and the diode junction resistance and capacitance are assumed constant. The resulting linear circuit is then solved by use of the Laplace transform to yield $V_j(t+\Delta t)$. The junction voltage, resistance, and capacitance are then incremented for the next time interval. Using this technique, with 1000 intervals per cycle, the steady-state solution is typically obtained within three complete LO cycles. Typical results for the diode voltages and currents (for a 1H1-type diode at 300 GHz) are shown in Fig. 8. Note

TABLE I
TYPICAL PARAMETERS FOR A 1H1 DIODE

T(K)	V_o(mV)	R_s(ohms)	C_{jo}(fF)	I_{sat}(A)
300	28	18	2.5	5×10^{-18}
20	10.5	21	2.5	2×10^{-48}

that when the forward current through junction resistance surpasses I_{FB}, the junction is assumed to be a short circuit. With knowledge of $V_j(t)$, the diode conductance and capacitance are determined and the matrix coefficients Y_{mn} are derived through numerical integrations of (19) and (20).

Following [13], we can define an augmented Y-matrix, which includes the diode series resistance as a part of the embedding network, yielding a matrix equation of the form

$$\begin{bmatrix} I_1' \\ I_0' \\ I_{-1}' \end{bmatrix} = \begin{bmatrix} Y_{11} + \dfrac{1}{R_s + Z_{RF}} & Y_{10} & Y_{1-1} \\ Y_{01} & Y_{00} + \dfrac{1}{R_s + Z_{IF}} & Y_{0-1} \\ Y_{-11} & Y_{-10} & Y_{-1-1} + \dfrac{1}{R_s + Z_{RF}} \end{bmatrix} \cdot \begin{bmatrix} V_1' \\ V_0' \\ V_{-1}' \end{bmatrix}. \tag{21}$$

This situation is depicted by the dashed line in Fig. 6. From [13], the conversion loss for this case is given by

$$L = \frac{|Z_{\mathrm{RF}} + R_s|^2 |Z_{\mathrm{IF}} + R_s|^2}{4|Z_{01}'|^2 \mathrm{Re}(Z_{\mathrm{RF}})\mathrm{Re}(Z_{\mathrm{IF}})} \tag{22}$$

where Z_{01}' is the 01 element of the inverse of the augmented Y-matrix.

Results from this analysis for a typical mixer diode, whose parameters are given in Table I, are shown in Fig. 9. The results shown are at an LO frequency of 300 GHz, where the dc bias value that yielded the lowest loss has been used.

These results indicate that the minimum conversion loss is approximately 5 dB at both room temperature and 20 K, again indicating that cryogenic cooling will not increase the conversion loss. However, in both cases, the total bias ($V_{\mathrm{LO}} + V_{\mathrm{dc}}$) required for minimum loss is greater than the flat-band potential. This demonstrates that allowing the diode to surpass the flat-band condition is beneficial despite the increase in junction capacitance that occurs as flat-band is approached.

V. DISCUSSION

The intrinsic conversion loss of a high-frequency mixer incorporating a small diameter Schottky-barrier mixer diode has been shown to decrease significantly when the diode is allowed to exceed the flat-band condition for part of the LO cycle. Furthermore, use of a numerical model of the mixer has shown that the minimum total conversion loss is achieved only if the diode is biased beyond flat-band. This is despite the increase in the junction capacitance that occurs as flat-band is approached. However, the conversion loss is not the final measure of the performance of a mixer. For this reason the mixer noise temperature[2] T_m must be discussed briefly. For the broad-band case, T_m can be expressed as [1]

$$T_m = (L - 2)T_{D,\mathrm{av}} \tag{23}$$

where $T_{D,\mathrm{av}}$ is a measure of the average diode noise temperature T_n through an LO cycle.

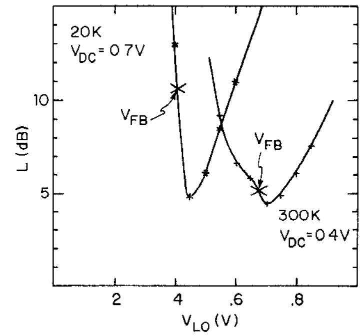

Fig. 9. Conversion loss versus V_{LO} for a 1H1 diode at 300 K and 20 K. In each case the dc bias which resulted in the lowest loss has been used. $Z_{\mathrm{RF}} = 100\ \Omega$ and a matched IF load have been assumed.

Fig. 10 presents a plot of the dc biased diode noise temperature T_n versus forward current for a typical mixer diode (type 1H1) at 300 K and 20 K. This data was measured at 1.4 GHz with a bandwidth of 100 MHz using a system described by Faber and Archer [22]. The sharp increase noted in the noise temperature at the higher currents is typical of all Schottky diodes and is commonly referred to as high field noise. The diode parameters, shown in Table I, along with (16) yield flat-band currents of approximately 2 mA and 0.5 mA at 300 K and 20 K, respectively. At these current levels, the high field noise begins to have an appreciable effect. Thus, any increase in the diode bias beyond the flat-band condition will increase the diode noise. However, the sharp decrease in the conversion loss at flat-band (Figs. 5 and 9) can outweigh the increase in $T_{D,\mathrm{av}}$ caused by the high field noise.

[2] Mixer noise temperature is defined as the increase in the temperature of the RF source that will produce the same noise in the matched IF load as do the noise sources in the mixer element.

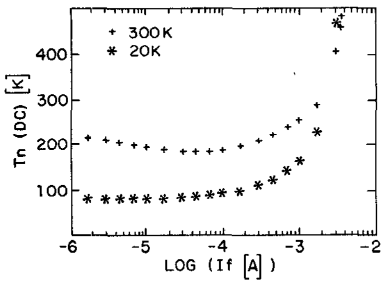

Fig. 10. DC biased equivalent noise temperature versus forward current for a 1H1 diode at 300 K and 20 K. Diode parameters are shown in Table I. Noise measurements have been supplied by Dr. M. Faber of the National Radio Astronomy Observatory [22].

Investigations of this very important tradeoff between conversion loss and diode noise rely on accurate modeling of the high field noise, which was not incorporated in previous mixer analyses [12], [13]. Recently, the affect of the high field noise on the mixer model was discussed by other authors [23]. Although this work has demonstrated a minimum value of T_m at high LO powers, the flat-band condition was not discussed. Detailed treatment of this effect will be reported in another paper [24].

VI. Summary and Conclusion

Conversion loss in Schottky-barrier mixer diodes can be modeled as the product of the intrinsic loss, caused by the nonideality of the junction conductance and the parasitic conversion loss caused by the parasitic series resistance and junction capacitance. Although the parasitic loss is difficult to model accurately, the intrinsic conversion loss sets a lower limit on the total conversion loss. Our investigation of intrinsic loss is similar to that of McColl [4]; however, we have used a more accurate model of the Schottky diode. This investigation has shown that cryogenic cooling improves, rather than degrades, the intrinsic conversion loss. Also, this analysis confirms that the intrinsic conversion loss will increase abruptly if the diode diameter is allowed to become very small. However, this effect becomes important at smaller diameters than previously predicted, and can be minimized if the diode doping is increased as the diode diameter is decreased. The previous intrinsic conversion-loss model neglected the effect of changes in diode doping.

Results from a recently developed numerical model of the conversion loss, which allows inclusion of the parasitic circuit elements, also indicate that cryogenic cooling will not degrade the conversion loss. This model, in agreement with the intrinsic conversion-loss model, predicts that the minimum conversion loss is obtained only if the diode exceeds the flat-band condition. This is despite the increase in the junction capacitance that occurs as flat-band is approached.

These results not only demonstrate the validity of the intrinsic conversion-loss model, but also give important insights into the performance of the mixer diode, and will have important implications for the design of future mixer diodes.

Acknowledgment

The authors wish to thank A. R. Kerr of the National Radio Astronomy Observatory in Charlottesville, VA, for his substantial contributions to this work.

References

[1] S. Weinreb and A. R. Kerr, "Cryogenic cooling of mixers for millimeter and centimeter wavelengths," *IEEE J. Solid State Circuits*, vol. SC-8, pp. 58–63, Feb. 1973.
[2] G. C. Messenger and C. T. McCoy, "Theory and operation of crystal diodes as mixers," *Proc. IRE*, vol. 45, pp. 1269–1283, Sept. 1957.
[3] A. R. Kerr, "Low-noise room temperature and cryogenic mixers for 80–120 GHz," *IEEE Trans. Microwave Theory Tech.*, vol. MTT-23, pp. 781–787, Oct. 1975.
[4] M. McColl, "Conversion loss limitations on Schottky barrier mixers," *IEEE Trans. Microwave Theory Tech.*, vol. MTT-25, pp. 54–59, Jan. 1977.
[5] H. C. Torrey and C. A. Whitmer, *Crystal Rectifiers*, (MIT Radiation Lab. Series, vol. 15). New York: McGraw-Hill, 1948.
[6] J. W. Archer, "All solid-state low-noise receivers for 210-240 GHz," *IEEE Trans. Microwave Theory Tech.*, vol. MTT-30, pp. 1247–1252, Aug. 1982.
[7] J. W. Archer and M. T. Faber, "Low-noise fixed tuned broadband mixer for 200–270 GHz," *Microwave J.*, pp. 135–142, July 1984.
[8] W. J. Wilson, "Submillimeter-wave receivers—A status report," *IEEE Trans. Microwave Theory Tech.*, vol. MTT-31, Nov. 1983.
[9] W. M. Kelly and G. T. Wrixon, "Schottky barrier diodes for low noise mixing in the far infrared," *Appl. Phys. Lett.*, vol. 32(9), pp. 525–527, May 1978.
[10] M. McColl, P. T. Hodges, and W. A. Garber, "Submillimeter-wave detection with submicron-size Schottky-barrier diodes," *IEEE Trans. Microwave Theory Tech.*, MTT-25, June 1977.
[11] B. J. Clifton, "Schottky-barrier diodes for submillimeter heterodyne detection," *IEEE Trans. Microwave Theory Tech.*, vol. MTT-25, pp. 457–463, June 1977.
[12] D. N. Held and A. R. Kerr, "Conversion loss and noise of microwave and millimeter-wave mixers: Part 1—Theory," and "Part 2—Experiment," *IEEE Trans. Microwave Theory Tech.*, vol. MTT-26, Feb. 1978.
[13] P. H. Siegel, A. R. Kerr, and W. Hwang, "Topics in the optimization of millimeter wave mixers," NASA Tech. Paper #2287, 1984.
[14] S. M. Sze, *Physics of Semiconductor Devices*, 2nd Ed. New York: Wiley and Sons, 1981, p. 255.
[15] J. A. Copeland, "Diode edge effect on doping-profile measurement," *IEEE Trans. Electron Devices*, vol. ED-17, May 1970.
[16] M. Pospieszalski and S. Weinreb, "A method of measuring an equivalent circuit of waveguide-mounted diodes," N.R.A.O. Electronics Division Internal Report No. 210, Oct. 1979.
[17] A. A. M. Saleh, *Theory of Resistive Mixers*., Cambridge, MA: The M.I.T. Press, 1971.
[18] F. A. Padovani and R. Stratton, "Field and thermionic field emission in Schottky barriers," Solid-State Electron., vol. 9, pp. 695–707, 1966.
[19] T. W. Crowe and R. J. Mattauch, "An analysis of the $I-V$ characteristics of cryogenically cooled Schottky-barrier mixer diodes," in *IEEE Southeastcon Proc.*, 1984, pp. 184–188.
[20] J. S. Blakemore, *Semiconductor Statistics*. New York: Pergamon Press, 1962.
[21] G. Stillman, University of Illinois, private communication.
[22] M. Faber and J. Archer, "Computer aided testing of mixers between 90 GHz and 350 GHz," *IEEE Trans. Microwave Theory Tech.*, vol. MTT-33, pp. 1138–1145, Nov. 85.
[23] G. Hegazi, A. Jelenski, and S. Yngvesson, "Limitations of microwave and millimeter-wave mixers due to excess noise," in *Proc. 1985 MTT Symposium*, pp. 431–434.
[24] T. Crowe and R. J. Mattauch, in preparation.

Thomas W. Crowe (S'86) received the B.S. degree (physics) from Montclair State College (NJ) in 1980. Since that time he has been at the University of Virginia Semiconductor Device Laboratory. He received the M.S.E.E. degree from UVa in 1982, and the Ph.D. degree in electrical engineering in January 1986.

He is presently a Research Associate at the University of Virginia. His main areas of interest are the development of high-frequency semiconductor devices and the optimization of mixer diodes for submillimeter wavelength receivers.

Dr. Crowe is a member of Sigma Xi and Eta Kappa Nu.

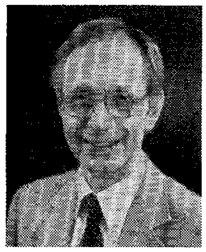

Robert J. Mattauch (S'61–M'66–SM'81–F'86) received the B.S.E.E. degree from the Carnegie Institute of Technology in 1962 and the M.E.E. and Ph.D. degrees in electrical engineering from North Carolina State University, Raleigh, in 1963 and 1967, respectively. He was a Ford Fellow at North Carolina State University.

His research interests lie in the area of semiconductor materials and devices, with specific emphasis on III-V compounds and millimeter-wave structures. He is presently a Wilson Professor of Electrical Engineering and Director of the Semiconductor Device Laboratory at the University of Virginia, Charlottesville.

Dr. Mattauch is a member of Eta Kappa Nu, Sigma Xi, Phi Kappa Phi, and Tau Beta Pi.